Spectrochimica Acta Part B 159 (2019) 105666

Contents lists available at ScienceDirect

Spectrochimica Acta Part B

journal homepage: www.elsevier.com/locate/sab

Analytical note

Improvement of palladium limit of detection by microwave-assisted laser induced breakdown spectroscopy

Ahlam A. Al Shuaili[1], Ahlam M. Al Hadhrami[1], M.A. Wakil, Zeyad T. Alwahabi*

School of Chemical Engineering, University of Adelaide, Adelaide, SA 5005, Australia

ARTICLE INFO

Keywords:
Laser-induced breakdown spectroscopy
Microwave assisted
Signal enhancement
Palladium detection

ABSTRACT

Detecting elements such as heavy metals is important in many industrial processes. The techniques currently used are time consuming and require excessive sample preparation. In this paper, we demonstrate microwave-assisted laser-induced breakdown spectroscopy (MW-LIBS) to detect palladium (Pd) in solid samples at ambient conditions. Microwave radiation was introduced by a near field applicator to couple the microwave radiation with the plasma. The results were a 92–fold enhancement in palladium signal with 8-fold improvement in the limit of detection at laser energy levels below 5 mJ (1250 J/cm^2 laser pulse fluence). We also investigate the optimum experimental parameters of palladium detection for both laser-induced breakdown spectroscopy (LIBS) and MW-LIBS. The maximum signal to noise ratio improvement was achieved at microwave power of 750 W and laser pulse fluence of 157 J/cm^2 for Pd I 340.46 nm. Finally, we examine the location of the near field applicator (NFA) with respect to the sample to show that the MW-LIBS signal strength was significantly affected by the vertical position compared to the horizontal. The detection limits of palladium with LIBS and MW-LIBS were 40 ppm and 5 ppm respectively.

1. Introduction

Element detection is a requirement in several industrial applications, including in the pharmaceutical, water treatment, mining and food industries. In the food industry, the detection of heavy metals is necessary to ensure that products are top quality, as heavy metals are a common contaminant [1]. Element detection also plays an important role in leaching, recovery and the recycling of precious metals or nuclear waste [2,3].

There are several techniques currently available for metal detection in industry. Some of the common techniques are induced coupled plasma spectroscopy ICP [4], atomic absorption [5] and X-ray fluorescents [6], which show outstanding results and extreme sensitivity. Despite their advantages, these techniques suffer from some common drawbacks; they are time consuming and require excessive sample preparation [7–12].

Laser-induced breakdown spectroscopy (LIBS) is an analytical technique in which a laser beam is used to detect elements directly from samples [13]. In the past decade, the application of LIBS has grown rapidly due to its real time analysis and the minimal preparation required, which lead to relatively fast measurements compared to other techniques [13]. LIBS has attracted interest in the industrial processes, as it is the ideal candidate for metal detection.

The disadvantages of LIBS include relatively low pulse to pulse repeatability, and low sensitivity [13,14]. To overcome these, several methods have been introduced. One of the most common techniques to increase the sensitivity of LIBS is the use of double pulse laser to create the plasma [2,14–17], which has attracted great interest due to its ability to enhance the signal as well as improve the limit of detection (LoD) [14]. Another common enhancing technique is the use of an additional source of energy to enhance the plasma of the element and to increase the sensitivity of detection [14]. These sources of secondary energy can be provided in many forms, such as resonant laser [18], spark discharge [19], stable flame [20], long pulse laser [21] and microwave-assisted laser-induced breakdown spectroscopy (MW-LIBS) [7–12,22].

MW-LIBS has been proven to enhance sensitivity by increasing the lifetime of the plasma [7–12,22]. The external energy supplied, using microwave radiation, sustains the free electrons present within the laser-induced plasma. These reenergized free electrons act as an excitation source, via collisional processes, extending the life of the short-lived laser-induced plasma. The coupling of microwave radiation with the plasma allows sufficient time for detection [11,8,12]. It has been shown recently that, by using MW-LIBS, the self-absorption issue can be

* Corresponding author.
E-mail address: zeyad.alwahabi@adelaide.edu.au (Z.T. Alwahabi).
[1] The first two authors contributed equally.

https://doi.org/10.1016/j.sab.2019.105666
Received 22 February 2019; Received in revised form 30 July 2019; Accepted 30 July 2019
Available online 01 August 2019
0584-8547/

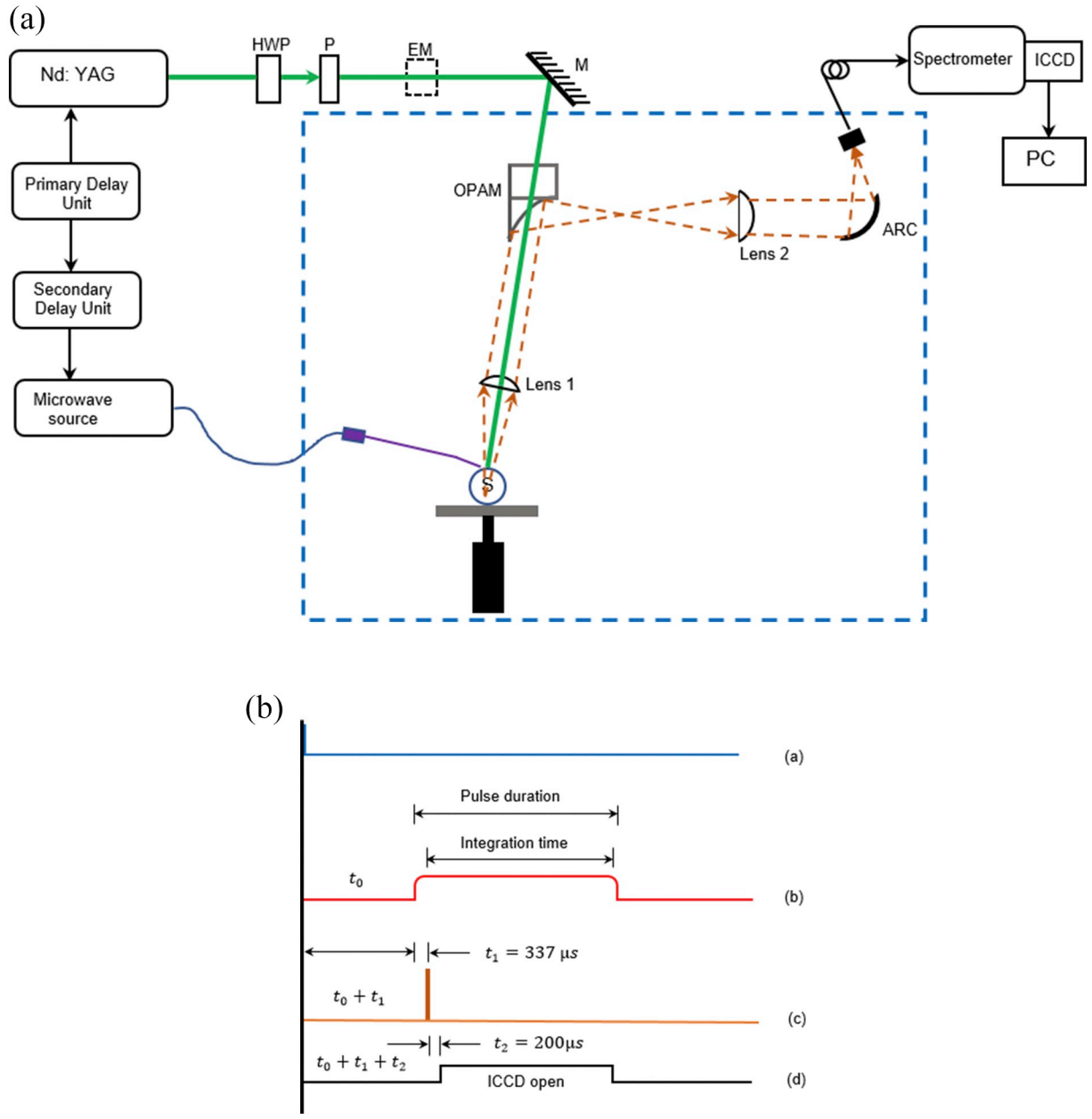

Fig. 1. (a): Schematic of the experimental setup, where HWP is halfwave plate, P is polarizer, EM is energy meter, M is mirror, OPAM is off-axis parabolic mirror, ARC is achromatic reflective coupler, and S is sample. (b): The timing diagram showing the primary pulse (t_0), a, the microwave trigger pulse, b, the laser trigger pulse, c, and the ICCD trigger pulse, d.

reduced significantly [11,23].

Several ways have been demonstrated to introduce MW power to the plasma, such as by using an enclosed cavity [8,10] or antenna [8,10,22], and most recently with a near field applicator (NFA) [11,12,24]. MW enhancement in the LoD using an enclosed cavity was 20-fold, 24-fold and 12.5-fold for copper [9], oxide calcium [25] and europium [10] respectively. The use of NFA at ambient condition achieved 93-fold and 11.5-fold improvements in the LoD for copper in solid samples [11] and indium in liquid traces [12] respectively.

To the best of our knowledge, MW-LIBS has not yet been demonstrated for palladium (Pd) detection. Palladium is a platinum group metal and it plays a key role in several industrial applications. Approximately 40% of automobile catalysts consist of palladium [26]; it is a cheaper alternative to the platinum fuel cell [27,28]. However, palladium is a limited natural resource and the cost of extracting and recycling it is high [29]. A sensitive detection method for palladium in the recyclable product would be valuable. Palladium detection is also useful in the pharmaceutical and food industries [30]. For example, palladium is used in some pharmaceutical tools. Here, detection of palladium is required due to the potential for severe health damage that may be caused by the complex biomolecules that are formed when palladium is combined with DNA and RNA [29]. A restriction limit of palladium contamination in the final product is strictly enforced.

Several studies have detected palladium by conventional LIBS. A study by Asimellis et al. [26] investigated palladium detection in a real automobile catalyst at a low concentration of 127 ppm, where several

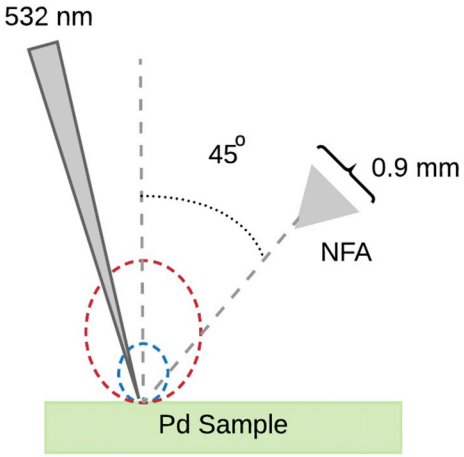

Fig. 2. Schematic presentation of the near field applicator (NFA) location related to the solid sample and the laser beam. The plasma without and with microwave is shown in blue and red respectively. (For interpretation of the references to colour in this figure legend, the reader is referred to the web version of this article.)

lines were observed for palladium detection, with high intensity lines at wavelengths of 340.46 nm and 342.12 nm [26]. Identical lines were also observed by Snyder et al. [28] where palladium was detected on a proton exchange membrane fuel cell in aqueous suspension [28]. Palladium was also detected in a bacterial cellulose membrane in both wet and dry matrices [31]. Here, the dry membrane was concluded to be the best matrix for palladium detection.

This paper demonstrates the effect of MW-LIBS in palladium spectral signals and the effect of various experimental parameters, such as MW power and laser pulse dependence, NFA position dependence, and line dependence of MW-LIBS on the signal enhancement.

2. Experimental set up

Several calibration samples containing a range of palladium concentrations (100 to 1000 ppm) were fabricated by mixing 0.1% palladium stock solution in 5 % HCl with 10 *wt.* % of sodium chloride solution and 5 *wt.* % of organic binder solution (polyethylene glycol). The additional water in the solutions was then evaporated at 250°C. The paste mixtures were transformed into a cylindrical uniform disc of 21 mm in diameter and 3.5 mm in thickness. The samples were dried at a temperature of 51 ° C for 20 min.

The experimental setup of MW-LIBS used for this work is presented schematically in Fig. 1(a). The 10 Hz, second harmonic output from a Q-switch Nd:YAG laser, Quantel (Brilliant B), ~6 ns was used. The pulse energy was controlled by a half-wave plate (HWP) and Glan-laser polarizer (P). The laser energy was measured with a Pyroelectric sensor (Thorlabs, ES 220C). The beam was focussed onto the sample surface using a fused silica lens (L1, with f = 100 mm). The spot size obtained at the focal point was estimated to be 140 μm^2 while the propagation of laser beam was at an angle of 15° to the verticle. To achieve the ablation from a fresh sample surface for each shot, the sample was placed on a rotating disk at 7 rotations per minute. A second CW laser, with a camera, was used to monitor the exact distance between the sample surface and L1. The timing diagram for the experiment is shown in Fig. 1(b).

A water cooled pulsed-microwave system operated at 2.45 GHz (Seirem), shown in the Fig. 1(a), was used. The microwave radiation was directed via a WR340 waveguide to a 3-stub impedance tuner and then to a waveguide-to-coaxial adaptor (WR340RN) through a quartz window. The waveguide-to-coaxial adaptor was connected to a 1 m flexible coaxial cable (50 Ω NN cable) with 0.14 dB @ 2.45 GHz. A semi rigid cable (RG402/U) was then connected at the end of the coaxial cable. The other end of the semi rigid cable was connected to a NFA, as was shown [11,32]. The NFA pointed tip was located at 45 ° with a distance of 0.5 mm vertically and horizontally from the solid sample, as shown in Fig. 2. A pulse generator (Aim-TTi) was used to control the microwave duration and power, and the microwave pulse was trigged prior to the laser pulse with a pulse duration of 1 ms.

The ablation beam was directed to pass through a perforated parabolic mirror (FL = 152 mm), then to focused by a plano-convex lens (FL = 100 mm), L1, onto the sample by a plano-convex UV fused silica lens with focal length of 100 mm and diameter 50.8 mm. The emission was collimated by L1 and then focused by an off-axis parabolic mirror (OPAM). A second lens L2 (FL = 20 mm) was used to couple the emission onto an Achromatic Reflective Coupler (ARC), which is connected to a 7-fibre bundle (Thorlabs, BFL200HS02). The fibre was

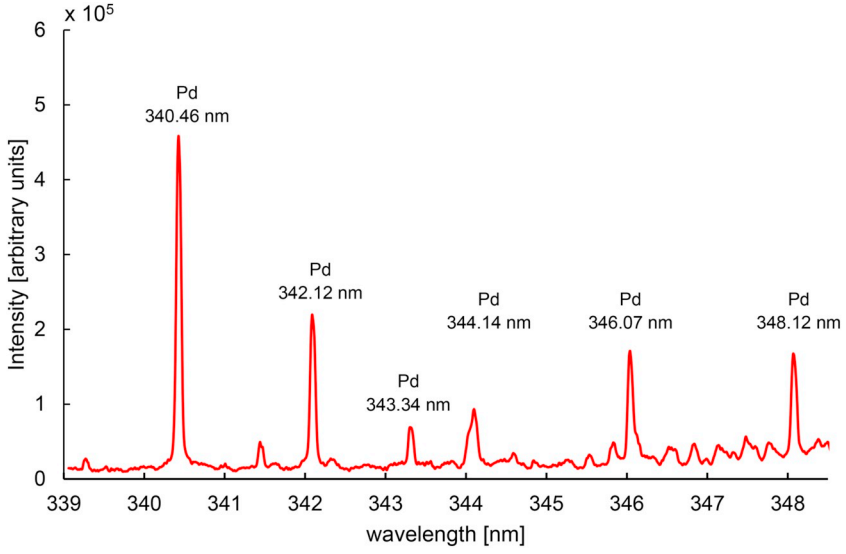

Fig. 3. Typical MW-LIBS spectra of 0.1 wt% Pd recorded at 1006 J/cm^2 laser fluence, 960 W microwave power, 450 ns gate-delay, 1 ms gate-width, and the spectral is for an accumulation of 100 shots.

Table 1
Summary of Pd I spectral lines in the present work [33].

Wavelength (nm)	Transition probability (s^{-1})	E_i (cm^{-1})	E_k (cm^{-1})	Lower level J_i	Upper level J_k
340.46	1.3×10^8	6564.148	35,927.948	3	4
342.12		7755.025	36,975.973	2	2
343.34		11,721.809	40,838.874	2	1
344.14		11,721.809	40,771.510	2	2
346.07	3.0×10^7	6564.148	35,451.443	3	3
348.977		11,721.8	40,368.796	2	1

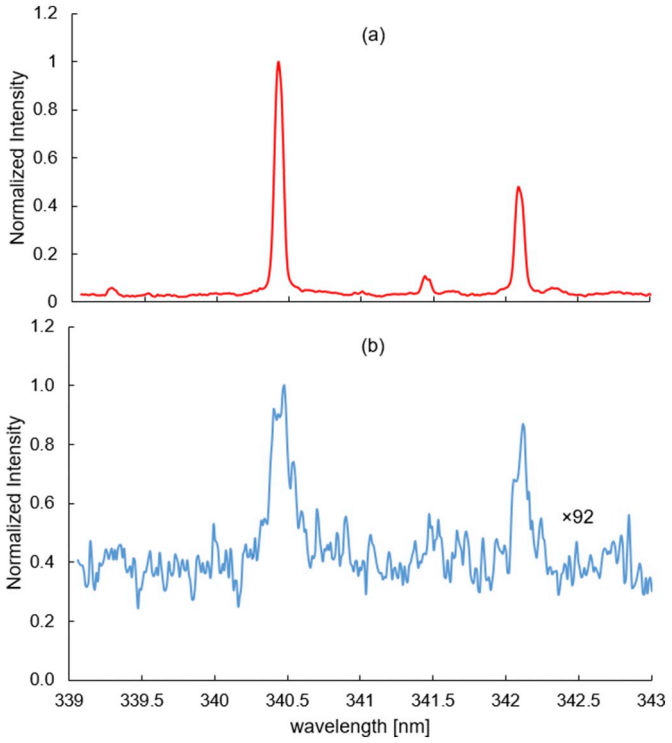

Fig. 4. Typical MW-LIBS, a, and LIBS, b, spectra of 0.08 wt% Pd, recorded at 650 J/cm^2 laser fluence, 960 W microwave power, 450 ns gate-delay and 1 ms gate-width for 100 shots. The intensity of the LIBS signal was multiplied by a factor of 92 for clarity.

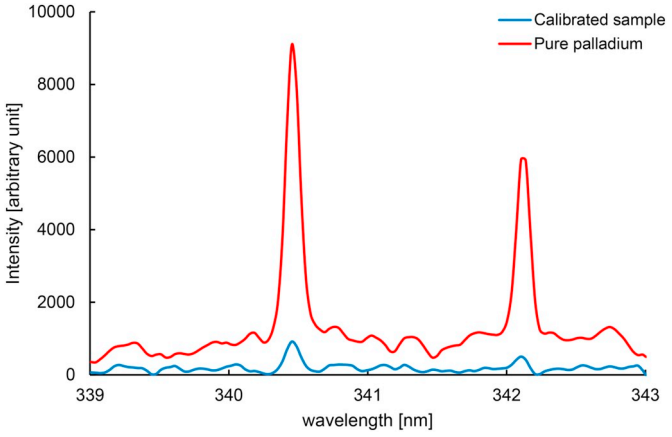

Fig. 5. Typical MW-LIBS spectra of pure sample (99 wt% Pd), red and calibrated sample (0.08 wt% Pd), blue, recorded at 650 J/cm^2 laser fluence, 960 W microwave power, 450 ns gate-delay, 1 ms gate-width for 100 shots. (For interpretation of the references to colour in this figure legend, the reader is referred to the web version of this article.)

connected to a spectrometer (Andor, Shamrock 500i with 2400 lines/mm grating) equipped with an intensifier camera, ICCD, (Andor, iStar). As shown in Fig. 1(a).

The optical line, sample holder, NFA and one end of the fibre were placed inside an aluminum box to minimize the residual microwave radiation, as shown in Fig. 1(a). One side of the aluminum box was covered with metal mesh acting as an observation window. The spectrometer (Andor Shamrock 500i) with a grating of 2400 lines/mm has a spectral resolving power of 10,000; that is, the spectral resolution is 0.031 nm in the spectral range of 320–332 nm. The maximum attainable wavelength range for the spectrometer, with the Holographic grating, is 200–705 nm. An intensified CCD camera (Andor, iStar) was used to record the spectral signal, which was synchronized with the laser and the microwave generator.

3. Results & discussion

Spectral emissions for both LIBS and MW-LIBS were recorded for palladium in the range of 339–350 nm where several lines were observed with various intensity, as shown in Fig. 3 and Table 1, which summarise the utilities' energy levels for each line. However, two transitions of palladium, namely 340.46 nm and 342.12 nm with the upper energy state of 35,927.948 cm^{-1} and 36,975.973 cm^{-1}, were selected for analyzing experimental parameters, though only 340.46 nm was used to calculate LoD (Fig. 4).

Fig. 5 demonstrates the spectral emissions for the 0.08 wt% palladium calibrated sample with the pure palladium sample (99 wt%) to validate the signal profile with the pure sample. Both samples show similar profiles with no variation in the signal at both 340.46 nm and 342.12 nm, which validates the accuracy of the measured calibrated sample.

The signal to noise ratio (SNR) improvement as a function of MW power at various laser fluences was measured for the palladium calibrated sample of 0.08 wt% and is shown in Fig. 6. The gate-delay and gate-width were kept at a fixed value of 450 ns and 1 ms respectively. Fig. 6 shows a linear increase of SNR improvement with increasing MW power, reaching a maximum near ~750 W and then a decrease with the increase of MW power after that point.

In relation to the laser fluence selected, Fig. 6 also shows that maximum SNR improvement can be achieved at MW power 750 W for each element. The maximum enhancement of the MW-LIBS can be achieved at the lowest laser fluence of 157 J/cm^2. This is due to the ease of MW power coupling at a lower fluence. Increasing the laser fluence will result in an increase in electron density of the plasma's core, which in turn will result in a reduction of MW power to penetrate to the plasma for the coupling and a measurement similar to that of a conventional LIBS [12,32]. The larger volume will reduce the influence of the MW to re-excite the core and instead it will excite the plasma fringes, as demonstrated by Chen et al. [32].

Fig. 7 shows the noise, signal enhancement and SNR improvement as a function of MW power. Note that increasing the MW power results in an increase in the signal enhancement until it reaches a maximum point and then starts to decrease. This may be related to the significant

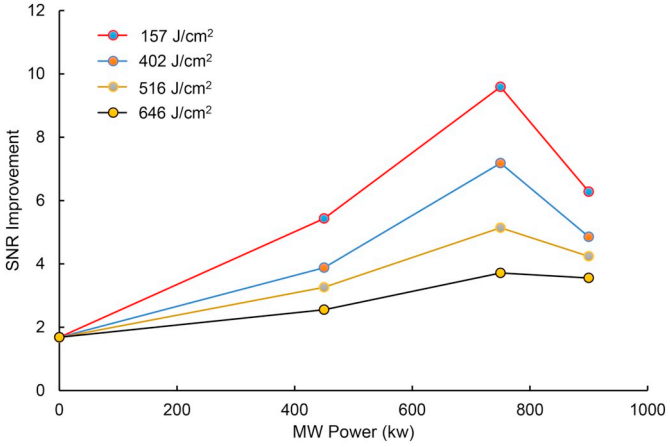

Fig. 6. Signal to noise ratio improvement of 0.08% Pd at a 450 ns gate-delay and 1 ms gate-width for 100 shots.

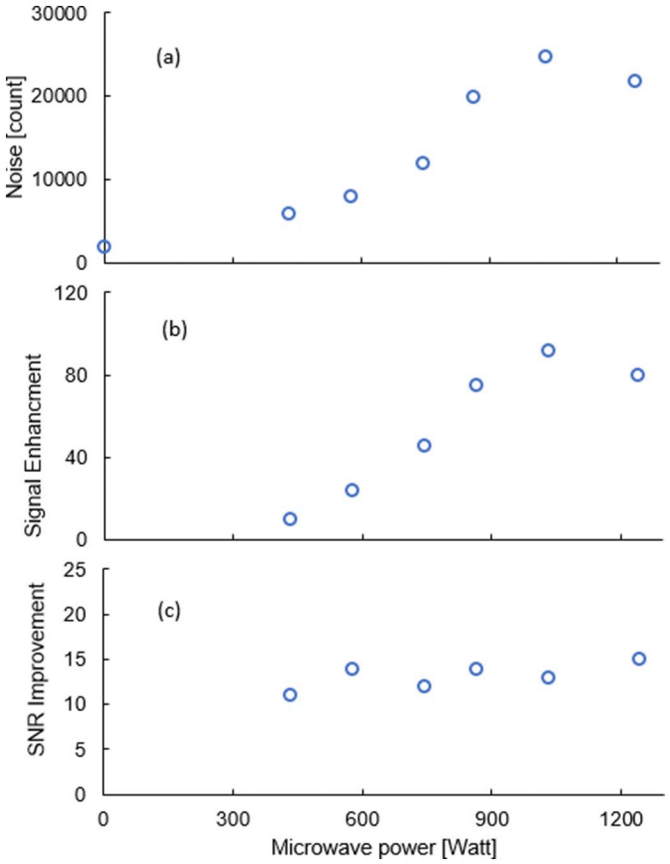

Fig. 7. The (a) noise level (counts), (b) signal enhancement, and (c) SNR improvement of 0.1 wt% Pd at laser pulse fluence of 650 J/cm^2, 450 ns gate-delay, 1 ms gate-width and an accumulation of 100 shots.

increase of the noise level at that stage, where increasing the MW power will significantly increase the noise level in addition to increasing the signal intensity. This is also shown in Fig. 7(c) as a nearly flat trend of the SNR improvement with the increase of MW power. This is due to the non-linear increase of the plasma's volume in relation to the MW power. It creates a non-stable plasma and a measurement that generates a significant noise level, as was noted by Iqbal et al. [24] for the study of the intensity and the plasma's volume as a function of MW power.

Another significant factor affecting MW power enhancement is the position of the NFA relative to the laser beam spot on the sample. The effect of signal enhancement as a function of NFA position both vertically and horizontally has been evaluated.

Fig. 8 represents the effect of the vertical and horizontal position on the signal intensity. A constant horizontal position of 0.4 mm was considered for the effect of vertical distance measurement, and a 0.7 mm vertical position was fixed for the horizontal distance measurement. Fig. 8 shows a significant sensitivity of signal intensity with both horizontal and vertical locations of NFA from the point of laser heating on the sample surface. Note that the signal intensity is significantly sensitive to the vertical location of the NFA compared to the horizontal position of the NFA. For each 0.1 mm change in vertical position of the NFA, the signal intensity drops significantly until it reaches the effect of convectional LIBS, where the decreasing trend of signal intensity with the horizontal distance is not so fast. This might be due to the actual shape of the palladium plasma. From the measurement, it appears that the shape is a horizontal oval where increasing the NFA distance vertically represents a measurement in the plasma fringes rather in the core. The increasing horizontal direction still allows the MW coupling since the NFA is still located in the plasma. The closer the NFA is to the sample, the higher the electric field, which produces higher enhancement of the signal due to higher coupling.

Fig. 9 shows the dependence of the signal intensity as a function of horizontal distance of the NFA at various vertical distances. The effect of the horizontal distance can be varied by increasing the vertical distance of the NFA from the laser beam. The signal intensity becomes more sensitive to the horizontal distance with the increase of the vertical position of the NFA, which might be due to the plasma dimensions and shape. In Fig. 9, it can also be seen that the optimum position for the MW power enhancement can be at the point of 0.7 mm vertical and 0.2 mm horizontally for the NFA position which is the point that represents the highest signal enhancement and the lowest noise level which was selected for the study carried.

Calibration of palladium in solid samples was done for both MW-LIBS and conventional LIBS under identical experimental conditions of 650 J/cm^2 laser pulse fluence, 750 W microwave power, 450 ns gate-delay and 1 ms gate-width. The quantitative detection was carried over the calibrated salt sample with various palladium concentrations. Fig. 10 represents the calibration curve for both LIBS and MW-LIBS, with linear fitting for the maximum intensity line of 340.46 nm. The slope of MW-LIBS is greater than the slope of LIBS only, which represents the increase in detection sensitivity with MW-LIBS. Detection increases almost the same as the increase in concentration of palladium in the sample, which corresponds to the accurate measurement and lower LoD obtained.

The LoD of palladium was calculated using Eq. (1):

$$LoD = \frac{k.\, s_i}{b} \tag{1}$$

where k is a constant (set to 3), s_i is the standard deviation of the background, and b is the slope of the calibration curve. It was found that the LoD is 40 ppm and 5 ppm for LIBS and MW-LIBS respectively. This leads to an 8-fold improvement in the LoD of palladium in solid samples. This improvement factor is within the range of previous quantitative MW-LIBS studies for solid phase [8–12,24,25]. As mentioned previously, palladium detection using LIBS has been investigated in several studies for both calibrating and mapping palladium samples unfortunately, even though some of the studies carried out were for quantitative measurement of palladium, there has not been a clear identification of LoD. Therefore, the LoD obtained for this study cannot be compared to others.

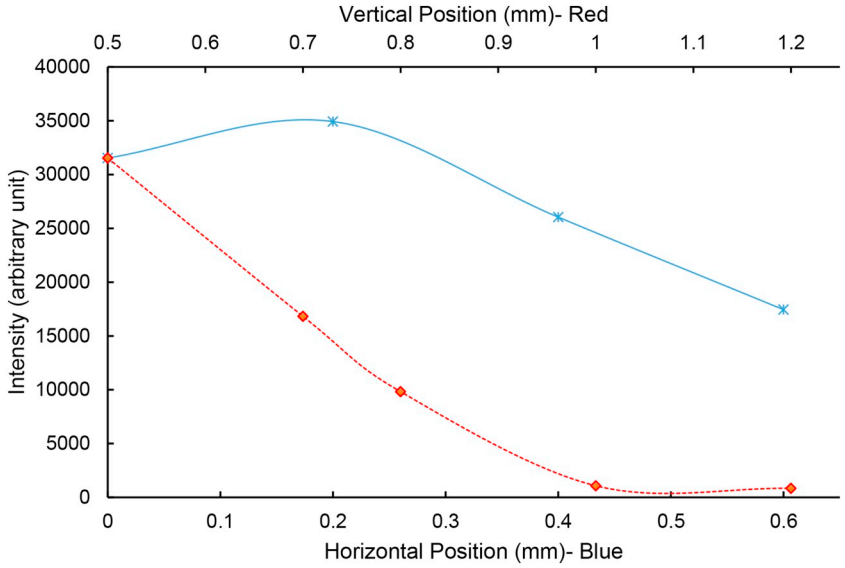

Fig. 8. The dependence of MW-LIBS signal intensity on the vertical distance of the NFA above the sample surface and the horizontal distance to the laser beam measured at 650 J/cm^2 laser fluence, 750 W microwave power, 450 ns gate-delay, 1 ms gate-width with an accumulation of 100 shots.

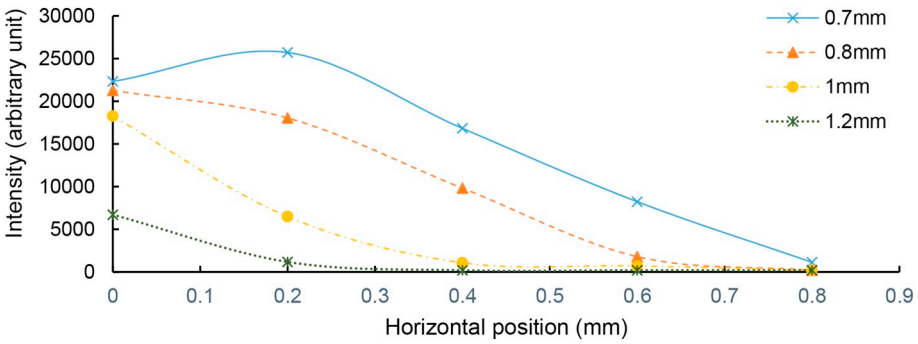

Fig. 9. Intensity as a function of horizontal position of the NFA, relative to the vertical position, indicated, of the NFA of 0.08 wt% Pd sample at 650 J/cm^2 laser fluence, 750 W microwave power, 450 ns gate-delay, 1 ms gate-width with the accumulation of 100 shots.

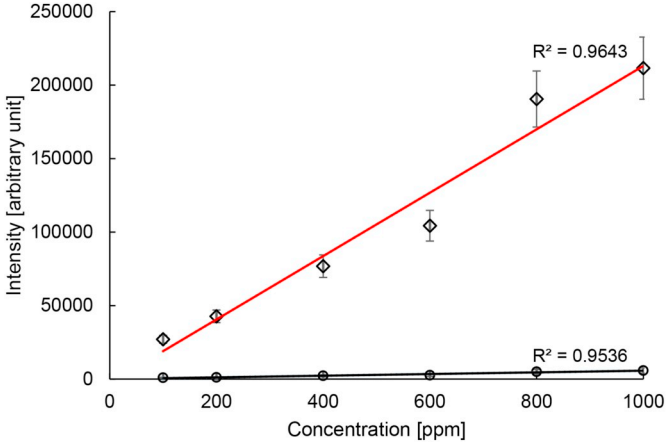

Fig. 10. Calibration curves of Pd (340.46 nm) with MW-LIBS, diamond, and LIBS, circle, at 650 J/cm^2 laser fluence, 750 W microwave power, 450 ns gate-delay, 1 ms gate-width. Error bars are standard deviation of 100 shots.

4. Conclusion

This study has demonstrated, for the first time, that MW-LIBS detects palladium in solid samples. We found that the signal was enhanced 92-fold with MW-LIBS, leading to an 8-fold improvement in LoD by MW-LIBS when compared with LIBS. The detection limit of palladium with LIBS and MW-LIBS were 40 ppm and 5 ppm respectively. The laser pulse fluence shows a maximum enhancement for the signal to noise at lower laser energy independent of the applied MW power. It was found that a point of maximum intensity is reached at a microwave power of 750 W. The position of NFA, was also demonstrated for the study to improve the LoD.

Novelty statement

We demonstrated for the first-time new LoD for Pd using an optimised-Microwave assisted Laser Induced Breakdown Spectroscopy. We achieved 11 folds improved in the detection sensitivity of Pd.

A new LoD of 5 ppm of Pd in sold sample was recorded using laser energy below 5 mJ.

References

[1] T. Balaji, S.A. El-Safty, H. Matsunaga, T. Hanaoka, F. Mizukami, Optical sensors based on nanostructured cage materials for the detection of toxic metal ions, Angew. Chem. 118 (2006) 7360–7366.
[2] K. Rifai, S. Laville, F. Vidal, M. Sabsabi, M. Chaker, Quantitative analysis of metallic traces in water-based liquids by UV-IR double-pulse laser-induced breakdown spectroscopy, J. Anal. At. Spectrom. 27 (2012) 276–283.
[3] O. Samek, D.C. Beddows, J. Kaiser, S.V. Kukhlevsky, M. Liska, H.H. Telle, A.J. Whitehouse, Application of laser-induced breakdown spectroscopy to in situ analysis of liquid samples, Opt. Eng. 39 (2000) 2248–2263.
[4] E. Herincs, M. Puschenreiter, W. Wenzel, A. Limbeck, A novel flow-injection method for simultaneous measurement of platinum (Pt), palladium (Pd) and rhodium (Rh) in aqueous soil extracts of contaminated soil by ICP-OES, J. Anal. At.

Spectrom. 28 (2013) 354–363.
[5] J.L. Molloy, J.A. Holcombe, Detection of palladium by cold atom solution atomic absorption, Anal. Chem. 78 (2006) 6634–6639.
[6] K. Van Meel, A. Smekens, M. Behets, P. Kazandjian, R. Van Grieken, Determination of platinum, palladium, and rhodium in automotive catalysts using high-energy secondary target X-ray fluorescence spectrometry, Anal. Chem. 79 (2007) 6383–6389.
[7] A. Khumaeni, K. Akaoka, M. Miyabe, I. Wakaida, The role of microwaves in the enhancement of laser-induced plasma emission, Front. Phys. 11 (2016) 114209.
[8] Y. Liu, M. Baudelet, M. Richardson, Elemental analysis by microwave-assisted laser-induced breakdown spectroscopy: evaluation on ceramics, J. Anal. At. Spectrom. 25 (2010) 1316–1323.
[9] Y. Liu, B. Bousquet, M. Baudelet, M. Richardson, Improvement of the sensitivity for the measurement of copper concentrations in soil by microwave-assisted laser-induced breakdown spectroscopy, Spectrochim. Acta B At. Spectrosc. 73 (2012) 89–92.
[10] M. Tampo, M. Miyabe, K. Akaoka, M. Oba, H. Ohba, Y. Maruyama, I. Wakaida, Enhancement of intensity in microwave-assisted laser-induced breakdown spectroscopy for remote analysis of nuclear fuel recycling, J. Anal. At. Spectrom. 29 (2014) 886–892.
[11] J. Viljanen, Z. Sun, Z.T. Alwahabi, Microwave assisted laser-induced breakdown spectroscopy at ambient conditions, Spectrochim. Acta B At. Spectrosc. 118 (2016) 29–36.
[12] M. Wall, Z. Sun, Z.T. Alwahabi, Quantitative detection of metallic traces in water-based liquids by microwave-assisted laser-induced breakdown spectroscopy, Opt. Express 24 (2016) 1507–1517.
[13] D.W. Hahn, N. Omenetto, Laser-induced breakdown spectroscopy (LIBS), part I: review of basic diagnostics and plasma–particle interactions: still-challenging issues within the analytical plasma community, Appl. Spectrosc. 64 (2010) 335A–366A.
[14] D.W. Hahn, N. Omenetto, Laser-induced breakdown spectroscopy (LIBS), part II: review of instrumental and methodological approaches to material analysis and applications to different fields, Appl. Spectrosc. 66 (2012) 347–419.
[15] V. Babushok, F. DeLucia Jr., J. Gottfried, C. Munson, A. Miziolek, Double pulse laser ablation and plasma: laser induced breakdown spectroscopy signal enhancement, Spectrochim. Acta B At. Spectrosc. 61 (2006) 999–1014.
[16] F. Colao, V. Lazic, R. Fantoni, S. Pershin, A comparison of single and double pulse laser-induced breakdown spectroscopy of aluminum samples, Spectrochim. Acta B At. Spectrosc. 57 (2002) 1167–1179.
[17] D.-H. Lee, S.-C. Han, T.-H. Kim, J.-I. Yun, Highly sensitive analysis of boron and lithium in aqueous solution using dual-pulse laser-induced breakdown spectroscopy, Anal. Chem. 83 (2011) 9456–9461.
[18] D. Cleveland, R.G. Michel, Quantitative analysis by resonant laser ablation with optical emission detection: resonant laser-induced breakdown spectroscopy, Microchem. J. 95 (2010) 120–123.
[19] O.A. Nassef, H.E. Elsayed-Ali, Spark discharge assisted laser induced breakdown spectroscopy, Spectrochim. Acta B At. Spectrosc. 60 (2005) 1564–1572.
[20] L. Liu, S. Li, X. He, X. Huang, C. Zhang, L. Fan, M. Wang, Y. Zhou, K. Chen, L. Jiang, Flame-enhanced laser-induced breakdown spectroscopy, Opt. Express 22 (2014) 7686–7693.
[21] D.K. Killinger, S.D. Allen, R.D. Waterbury, C. Stefano, E.L. Dottery, Enhancement of Nd: YAG LIBS emission of a remote target using a simultaneous CO 2 laser pulse, Opt. Express 15 (2007) 12905–12915.
[22] A. Khumaeni, M. Miyabe, K. Akaoka, I. Wakaida, The effect of ambient gas on measurements with microwave-assisted laser-induced plasmas in MA-LIBS with relevance for the analysis of nuclear fuel, J. Radioanal. Nucl. Chem. 311 (2017) 77–84.
[23] Y. Tang, J. Li, Z. Hao, S. Tang, Z. Zhu, L. Guo, X. Li, X. Zeng, J. Duan, Y. Lu, Multielemental self-absorption reduction in laser-induced breakdown spectroscopy by using microwave-assisted excitation, Opt. Express 26 (2018) 12121–12130.
[24] A. Iqbal, Z. Sun, M. Wall, Z.T. Alwahabi, Sensitive elemental detection using microwave-assisted laser-induced breakdown imaging, Spectrochim. Acta B At. Spectrosc. 136 (2017) 16–22.
[25] A. Khumaeni, T. Motonobu, A. Katsuaki, M. Masabumi, W. Ikuo, Enhancement of LIBS emission using antenna-coupled microwave, Opt. Express 21 (2013) 29755–29768.
[26] G. Asimellis, N. Michos, I. Fasaki, M. Kompitsas, Platinum group metals bulk analysis in automobile catalyst recycling material by laser-induced breakdown spectroscopy, Spectrochim. Acta B At. Spectrosc. 63 (2008) 1338–1343.
[27] E. Antolini, Palladium in fuel cell catalysis, Energy Environ. Sci. 2 (2009) 915–931.
[28] S.C. Snyder, W.G. Wickun, J.M. Mode, B.D. Gurney, F.G. Michels, The detection of palladium particles in proton exchange membrane fuel-cell water by laser-induced breakdown spectroscopy (LIBS), Appl. Spectrosc. 65 (2011) 642–647.
[29] B. Liu, H. Wang, T. Wang, Y. Bao, F. Du, J. Tian, Q. Li, R. Bai, A new ratiometric ESIPT sensor for detection of palladium species in aqueous solution, Chem. Commun. 48 (2012) 2867–2869.
[30] C.E. Garrett, K. Prasad, The art of meeting palladium specifications in active pharmaceutical ingredients produced by Pd-catalyzed reactions, Adv. Synth. Catal. 346 (2004) 889–900.
[31] M. Martin, B. Evans, H. O'Neill, J. Woodward, Laser-induced breakdown spectroscopy used to detect palladium and silver metal dispersed in bacterial cellulose membranes, Appl. Opt. 42 (2003) 6174–6178.
[32] S.J. Chen, A. Iqbal, M. Wall, C. Fumeaux, Z.T. Alwahabi, Design and application of near-field applicators for efficient microwave-assisted laser-induced breakdown spectroscopy, J. Anal. At. Spectrom. 32 (2017) 1508–1518.
[33] S.G. Johnson, NIST Standard Reference Database Journal of Physical and Chemical Reference Data Reprints, Energy 41 (2012).